

The BMP4-Smad Signaling Pathway Regulates Hyperandrogenism Development in a Female Mouse Model

Yang Liu^{1,2}, Shao-Yue Du¹, Meng Ding², Xin Dou², Fei-Fei Zhang¹, Zhi-Yong Wu¹, Shu-Wen Qian², Wei Zhang¹, Qi-Qun Tang^{2#}, Cong-Jian Xu^{1#}

¹Shanghai Key Laboratory of Female Reproductive Endocrine Related Disease, Obstetrics and Gynecology Hospital, Fudan University, Shanghai 200090, PR China;

²Key Laboratory of Metabolism and Molecular Medicine, the Ministry of Education; Department of Biochemistry and Molecular Biology, Fudan University Shanghai Medical College, Shanghai 200032, PR China

Running title: BMP4 Inhibited Hyperandrogenism Occurrence

Keywords: endocrinology; polycystic ovary syndrome; hyperandrogenism; androgen; BMP; Smad transcription factor; cytochrome P450

#To whom correspondence should be addressed:

Dr. Qi-Qun Tang, Key Laboratory of Metabolism and Molecular Medicine, the Ministry of Education; Department of Biochemistry and Molecular Biology, Fudan University Shanghai Medical College, Shanghai 200032, PR China

Tel: 86-21-54237198; Fax: 86-21-54237290; E-mail: qqtang@shmu.edu.cn

Dr. Cong-Jian Xu, Department of Gynecology, Obstetrics and Gynecology Hospital of Fudan University, 419 Fangxie Road, Shanghai, 200011 PR China

E-mail: xucj@hotmail.com.

Yang Liu and Shao-Yue Du contributed equally to this study.

Abstract

Polycystic ovary syndrome (PCOS) is a common endocrine disorder and a major cause of anovulatory sterility in women at reproductive age. Most patients with PCOS have hyperandrogenism, caused by excess androgen synthesis. Bone morphogenetic protein 4 (BMP4) is an essential regulator of embryonic development and organ formation, and recent studies have also shown that BMP4 may be involved in female steroidogenesis process. However, effect of BMP4 on hyperandrogenism remains unknown. Here, using a female mouse model of hyperandrogenism, we found that ovarian BMP4 levels were significantly decreased in hyperandrogenism. Elevated

androgens inhibited BMP4 expression via activation of androgen receptors. Moreover, BMP4 treatment suppressed androgen synthesis in theca cells and promoted estrogen production in granulosa cells, by regulating the expression of steroidogenic enzymes, including *CYP11A*, *HSD3B2*, *CYP17A1* and *CYP19A1*. Consistently, knockdown of BMP4 augmented androgen level and inhibited estrogen level. Mechanistically, Smad signaling rather than the p38 MAPK pathway regulated androgen and estrogen formation, thereby mediating the effect of BMP4. Of note, BMP4-transgenic mice were protected against hyperandrogenism. Our observations clarify a vital role of BMP4 in controlling sex hormone levels, and offer new insights into

intervention for managing hyperandrogenism by targeting the BMP4-Smad signaling pathway.

Introduction

Polycystic ovary syndrome (PCOS) is a highly heterogeneous and multifactorial endocrine disorder, which is the leading cause of non-ovulation infertility in women of reproductive age (1-2). Generally, PCOS is mainly characterized by two out of the following three criteria: oligo-ovulation or non-ovulation, clinical/biochemical hyperandrogenism and polycystic ovary appearance on ultrasonography. Its global prevalence is estimated to be between 6% and 10% and even up to 21%, depending on the diagnostic criteria and geographic location (3).

Hyperandrogenism is a key feature of PCOS and contributes to the clinical phenotype of PCOS patients, including menstrual and ovulatory dysfunction, hirsutism, and acne (4-5). This condition is characterized by elevated serum level of androgens such as testosterone, dihydrotestosterone and dehydroepiandrosterone (DHEA), primarily due to excess androgens production. In females, androgens are synthesized *de novo* from cholesterol in the ovarian theca cells (TCs) and the adrenal cortex. The ovarian TCs are stimulated by luteinizing hormone (LH) or insulin, which in turn activate series of steroidogenic enzymes, including cytochrome P450_{scc} (encoded by *CYP11A*), Δ^5 -isomerase- 3β -hydroxysteroid dehydrogenase type 2 (3β HSD2, encoded by *HSD3B2*) and P450_{c17} (encoded by *CYP17A1*), thereby catalyzing the synthesis of androgens including testosterone and dihydrotestosterone (6-7). The newly synthesized androgens then in part diffuse from TCs to granulosa cells (GCs), where they are aromatized by cytochrome P450_{arom} (encoded by *CYP19A1*) to produce estrogens such as estrone and estradiol (6-8). These steroidogenic enzymes are essential to the level of sex hormones. Therefore, genetic mutation or

aberrant expression of these genes may be highly related to pathogenesis of hyperandrogenism and PCOS (9). It is reported that the rate-limiting enzyme P450_{c17} is highly expressed and activated in ovarian TCs of PCOS patients, giving rise to increased androgens formation (10-11). Thus, to investigate the steroidogenesis process and the regulation of steroidogenic enzymes are necessary to understand the molecular basis underlying hyperandrogenism and PCOS development.

Bone morphogenetic protein-4 (BMP4) is a secreted protein and belongs to the bone morphogenetic protein family (12). It is well-established that BMP4 plays a vital role in embryonic development and organ formation (13). BMP4, like other BMP family members, elicit their effects through two distinct serine-threonine kinase transmembrane receptors, type I and type II receptors (12,14). Once binding with BMP4, type I receptors are activated, and in turn transduce intracellular signals via mothers against dpp (Smad) and p38 mitogen-activated protein kinase (MAPK) pathway. In the former case, activated BMP type I receptors phosphorylate receptor-regulated Smads (R-Smads) at their carboxy-terminal S-S-X-S motifs, including Smad1, Smad5, and Smad8, which are BMP-specific R-Smads. The phosphorylated and activated R-Smad proteins form complexes with common partner Smad (coSmad), that is, Smad4, the BMP-specific coSmad. Smad complexes containing one Smad4 and two R-Smads move into the nucleus and associate with various transcriptional co-activators or co-repressors, then bind to regulatory elements of target genes to regulate their transcription (12,14). In addition to Smad, p38 MAPK mediates BMP4 function in such physiological processes as cell differentiation and organ development. Upon phosphorylation by type I receptors, TGF-beta activated kinase 1 (TAK1) recruits TAK1-binding protein 1, and initiates phosphorylation cascade with MAPK

kinase kinase (MKK) and p38 MAPK. Phosphorylated/activated p38 MAPK then activates the expression of BMP-target genes (12,14).

We previously reported that BMP4 was required for commitment from pluripotent stem cells to the adipocyte lineage (15-16); and that BMP4 could improve systemic insulin sensitivity and energy homeostasis (17). The effect of BMP4 on metabolic improvement indicated its potential role in regulating PCOS and hyperandrogenism, as increasing evidence showed that hyperandrogenism was highly related with metabolic disorders (18). Additionally, it has been reported that BMPs promoted primordial follicle development (19) and might be involved in ovarian steroidogenesis process *in vitro* (20-21). However, the effect of BMP4 on androgens production is still controversial and the underlying molecular mechanism needs further clarification. In the current study, we investigated the effect of BMP4 on coordination between androgen and estrogen synthesis; and shed light on the mechanism underlying the regulation of steroidogenic enzymes by BMP4. Our results emphasized the essential role of BMP4-Smad signaling pathway in the regulation of hyperandrogenism development.

Results

BMP4 expression in ovary was negatively related with the occurrence of hyperandrogenism

In order to clarify the expression of BMP4 on hyperandrogenism pathogenesis, we established PCOS mice model by consecutively injecting mice with DHEA for 20 days. Abnormal estrous cycles (Fig. 1A), dropsical ovary and uterus (Fig. 1B), increased cystic follicles (Fig. 1C), and elevated serum testosterone (Fig. 1D) were found in DHEA-treated mice, indicating that PCOS model was successfully developed. We

therefore detected BMP4 expression in ovaries, finding out that both mRNA and protein levels of BMP4 were significantly decreased in hyperandrogenism ovaries compared with control (Fig. 1E-F).

In addition to BMP4, we found that part of BMP family members were downregulated in hyperandrogenism ovaries, including *BMP5*, *BMP6*, *BMP8b*, *BMP11*, *BMP12*, and *BMP15* (Supplemental Fig. 1A), suggesting that BMP signaling might be impaired in hyperandrogenism. We also detected the expression of BMP antagonists and found that mRNA levels of *Noggin*, *Chordin*, *Follistatin* and *Gremlin* were not affected in hyperandrogenism condition (Supplemental Fig. 1B).

Androgens inhibited BMP4 expression via androgen receptor (AR)

To identify the cell types that contributed to the downregulated BMP4 expression, we isolated ovarian TCs and GCs. Consistent with previous report (22), BMP4 was mainly expressed in TCs (Fig. 2A). We then treated TCs and GCs with testosterone and DHEA. qPCR assay showed that both testosterone and DHEA induction could repress BMP4 expression in TCs and GCs (Fig. 2B-C). As several androgen response elements were found in BMP4 promoter (data not shown), we then sought to confirm whether androgens regulated BMP4 promoter activity. To this end, we conducted reporter assays by inserting BMP4 promoter to the upstream of *luciferase* gene. We observed that BMP4 promoter activity was significantly inhibited by testosterone and DHEA treatment in a dose-dependent manner (Fig. 2D). Based on the notion that androgens function through AR activation (23), we therefore determined whether AR regulated BMP4 expression. We found that deficiency of AR significantly reversed the downregulated BMP4 expression caused by testosterone (Fig. 2E); and that AR could significantly attenuate BMP4

promoter activity (Fig. 2F). We then performed Chromatin immunoprecipitation (ChIP) assay in TCs and GCs. ChIP-qPCR analysis showed that AR could bind to BMP4 promoter upon testosterone treatment (Fig. 2G). These results collectively illustrated that BMP4 was downregulated by androgens through AR.

BMP4 inhibited androgen synthesis and promoted estrogen production

It is well-established that androgens were mainly synthesized in ovarian TCs and estrogens were produced in GCs (9). We therefore isolated TCs and GCs and treated them with BMP4, finding out that total testosterone from TCs supernatant was significantly decreased by BMP4 in a dose-dependent manner, whereas estrogen level from GCs supernatant was elevated (Fig. 3A). Then we detected expression of several steroidogenic enzymes, including *CYP11A*, *HSD3B2* and *CYP17A1*, which were responsible for androgens synthesis in TCs, as well as *CYP19A1*, which was critical for estrogen formation in GCs (Fig. 3B). We found that mRNA levels of enzymes for androgen production in TCs, especially *CYP17A1*, was significantly suppressed by BMP4 treatment; and that *CYP19A1* in GCs was dramatically promoted by BMP4 (Fig. 3C). However, expression of SF1, a known transcription factor of *CYP17A1* and *CYP19A1* (24), was not affected by BMP4 (Fig. 3C). Consistently, CYP17A1 protein level in TCs was decreased and CYP19A1 protein level in GCs was increased by BMP4 (Fig. 3D). We then investigated the effect of Noggin on steroidogenic enzymes expression, which is a well-known antagonist for BMP4 (25). We found that Noggin significantly reversed the altered steroidogenic genes expression caused by BMP4 in both TCs and GCs (Fig. 3E). In brief, Noggin augmented expression of *CYP11A*, *HSD3B2*, and *CYP17A1* in TCs, and repressed expression of *CYP19A1* in GCs.

We then disrupted BMP4 expression by adenovirus and measured androgen and estrogen production. We found that knockdown of BMP4 promoted androgen synthesis in TCs and inhibited estrogen in GCs (Fig. 4A). Consistently, knockdown of BMP4 augmented *CYP11A*, *HSD3B2*, and *CYP17A1* expression in TCs, while repressed *CYP19A1* expression in GCs (Fig. 4B). Taken together, these data suggested that BMP4 inhibited androgens synthesis in ovarian TCs and promoted estrogens production in GCs.

BMP4 activated both Smad and p38 MAPK signaling pathway in TCs and GCs

BMP4 binds to two distinct type I and type II serine/threonine kinase receptors, which activates Smad and p38 MAPK signaling pathway, thereby regulating cellular processes (12,14). We found that ovarian TCs and GCs mainly expressed type I receptor Bmpr1a and the type II receptors Bmpr2 and Acvr2a, indicating that these cells might be the direct target of BMP4 (Fig. 5A). Additionally, western blot showed that BMP4 activated both Smad and p38 MAPK pathway in TCs and GCs, as indicated by increased phosphorylated (p)-Smad1/5/8 and p-p38 MAPK (Fig. 5B).

Smad signaling was required for the effect of BMP4 on androgen and estrogen production

The data above implied that both Smad and p38 MAPK signaling pathway were activated by BMP4 in TCs and GCs. To explore which pathway mediated BMP4's effect, we respectively disrupted Smad4 and p38 MAPK expression by using two sets of siRNA. Smad4 is BMP4-specific coSmad, which is required for Smad complex formation to regulate target genes (12,14). Hence, Smad signaling could be disrupted upon Smad4 deficiency. We found that knockdown of Smad4 by siSmad4-1 and siSmad4-2 increased total testosterone level secreted by TCs and decreased estrogen level

from GCs, even under the condition of BMP4 treatment (Fig. 6A). In contrast, knockdown of p38 MAPK had little effect on androgen and estrogen levels, and even slightly increased estrogen level in GCs (Fig. 6A). We then detected expression of steroidogenic enzymes and found that Smad4-deficiency could reverse BMP4-induced expression changes of these enzymes. Briefly, deficiency of Smad4 promoted *CYP11A*, *HSD3B2* and *CYP17A1* expression in TCs, and inhibited *CYP19A1* in GCs, while disruption of p38 MAPK could hardly affect these (Fig. 6B and C). Collectively, these results suggested that Smad pathway, instead of p38 MAPK, mediated BMP4 function in regulating androgens and estrogens synthesis.

The results above indicated that BMP4 regulated *CYP17A1* expression through Smad signaling pathway, which motivated the hypothesis whether Smad protein directly modulated promoter activity of *CYP17A1*. To test the possibility, we transfected *CYP17A1* promoter into 293T cells with Smad1 or Smad4, and reporter assay was then performed, finding out that both Smad1 and Smad4 repressed *CYP17A1* promoter activity in a dose-dependent manner (Fig. 6D). We further carried out reporter assay in TCs, with the same results (Fig. 6E). These results together indicated that Smads could regulate *CYP17A1* expression.

BMP4-transgenic mice were protected against hyperandrogenism development

We then sought to demonstrate the effect of BMP4 *in vivo*. Since the adipose tissue is the main source of BMP4, we generated adipocyte-specific BMP4-transgenic (BMP4-TG) mice. As DHEA-treatment might conceal the possible changes of androgen level caused by BMP4, we established PCOS model on BMP4-TG mice by injecting insulin and hCG for 3 weeks as described (Fig. 7A), which was a well-acknowledged method to generate endogenous hyperandrogenism (26). No

significant weight changes were observed between BMP4-TG and WT mice (Fig. 7B). Intriguingly, WT mice developed abnormal estrous cycles upon induction, while BMP4-TG mice underwent normal estrous cycles (Fig. 7C). Of note, the serum testosterone of BMP4-TG mice was significantly lower than WT mice (Fig. 7D), while no significant difference was found in estrogen level (Fig. 7D). Consistently, decreased *CYP17A1* level and increased *CYP19A1* level were observed in the ovaries of BMP4-TG mice compared with WT mice (Fig. 7E). These results together suggested that BMP4 inhibited hyperandrogenism development, which validated the results *in vitro*.

Discussion

In the current study, we found that BMP4 was downregulated by high level of androgens. BMP4 treatment inhibited androgens synthesis in ovarian TCs and promoted estrogens production in GCs. The molecular mechanism is that BMP4 activated Smad signaling pathway, which in turn inhibited expression of *CYP17A1*. Based on these findings, we proposed a model in which BMP4 plays a role in controlling hyperandrogenism development by regulating androgens synthesis (Fig. 8). In normal, BMP4 coordinated the androgen and estrogen synthesis in ovary through Smad pathway. In the condition of androgen excess, ovarian BMP4 expression was suppressed by activated AR. The negative regulation of androgen synthesis was then relieved as a consequence of downregulated BMP4; therefore, androgen production was further increased and the hyperandrogenism eventually developed (Fig. 8). The negative feedback loop between BMP4 and androgen synthesis was critical for hyperandrogenism occurrence.

In addition to endocrine dysfunction, hyperandrogenism and PCOS are closely related to metabolic syndrome, including obesity, insulin resistance, type 2 diabetes and hyperlipidemia

(18). It is estimated that among PCOS patients, 50%-75% develop overweight or diabetes, and about 70% manifest insulin resistance (27). As a consequence of insulin resistance, insulin secretion is compensatorily augmented and contributes to hyperinsulinaemia. High level insulin associates synergistically with LH and activates P450c17, in turn promotes production and release of androgens (27). The role of insulin resistance and hyperinsulinaemia in the occurrence of PCOS is supported by observations that improving insulin sensitivity through weight loss or drug therapy such as metformin treatment ameliorates metabolic, hyperandrogenic, and reproductive features of PCOS (28). We previously found that BMP4 improved systemic insulin sensitivity and energy homeostasis (17). In combination with our current finding that BMP4 prevented body from hyperandrogenism, it emphasizes the conception that hyperandrogenism is highly related with energy metabolism. Therefore, to identify the essential regulator for the coordination between metabolic conditions and hyperandrogenism may not only clarify the mechanisms underlying PCOS pathogenesis but also provide new strategies for PCOS treatment.

Regulation of BMP4 expression has seldom been studied so far. We found for the first time that testosterone and DHEA inhibited BMP4 expression through suppressing its promoter activity. It is well-acknowledged that androgens exert their genomic effects via interaction with AR (23). AR is a ligand-dependent nuclear transcription factor and belongs to the steroid hormone nuclear receptor family. In the absence of androgens, AR associates with chaperone proteins, and keeps cytoplasmic (29). Upon binding with the ligands, AR dissociates itself from chaperone proteins, exposes the nuclear localization signal domain, and translocates to the nucleus, where it binds to androgen response elements and regulates target gene transcription (29). Here we found that AR bound to BMP4

promoter and inhibited BMP4 promoter activity, thereby repressing its expression. However, the underlying mechanism remains unknown. It is reported that the transcriptional activity of AR is modulated by specific co-activator or co-repressor (30). The best-studied AR corepressors so far are nuclear receptor corepressor (NCoR) and silencing mediator of retinoid and thyroid hormone receptors (SMRT) (31). AR could directly bind with NCoR and SMRT (32). Repression transcription of NCoR/SMRT complex is mediated through recruitment of histone deacetylases (31). Therefore, it is of interest to investigate whether NCoR/SMRT complex or other corepressors are involved in AR-mediated regulation of BMP4 expression.

BMP4 acts through two types of signaling pathway, Smad and p38 MAPK pathway (12,14). Smad and p38 MAPK seem to mediate distinct functions of BMP4. It is well-known that Smad4 associates with R-Smad complexes and co-translocates into the nuclei, where they recruit co-factors to regulate target gene expression. BMP4-specific Smad complexes could not be assembled upon Smad4 ablation; therefore Smad signaling transduction was reduced (12,14). In the current study, disruption of Smad signaling, but not p38 MAPK, reversed BMP4's effect on androgen and estrogen synthesis. On the contrary, knockdown of p38 MAPK slightly augmented estrogen level, probably due to the mild increase of CYP19A1 expression (Fig. 6B and C). We then found that Smad inhibited *CYP17A1* promoter activity, thereby repressed *CYP17A1* expression. We also found that CYP19A1 expression was regulated by BMP4-Smad signaling, the underlying mechanism of which needs further investigation. Our observation indicated that BMP4-Smad pathway is a negative regulator of androgen synthesis, which is an essential process in PCOS development. Interestingly, a recent report echoes our findings (33). It has been reported that disruption of

Smad4 signaling in the ovary causes premature GC luteinization and impaired ovulation and cumulus expansion (33). Hence, BMP4-Smad signaling pathway might be a potential target for PCOS intervention.

Besides BMP4, other BMPs have been showed to regulate hormone synthesis, including BMP2, BMP6, BMP7 and BMP15. For instance, BMP6 and BMP7 enhanced both basal and stimulated secretion of estradiol, while repressed progesterone in GCs (34). It is reported that BMP6 and BMP7 inhibited basal and LH-induced androgen production by bovine theca interna cells (20), although the underlying mechanisms have not yet been clarified. It seems that BMP family members exert similar function in modulating ovarian steroidogenesis. Therefore, ovarian BMP signaling defect may be a leading cause for hyperandrogenic dysfunction, suggesting BMP-Smad pathway as a potential target for hyperandrogenism treatment.

Experimental procedures

Animals and establishment of PCOS mice model

Female C57BL/6J mice were purchased from the Model Animal Research Center of Nanjing University. To establish the PCOS model, 4-week-old mice were injected daily (s.c.) with DHEA (6 mg/100 g body weight) dissolved in camellia oil for 20 consecutive days, with camellia oil injection as the control. Mice estrous cycle was assessed by vaginal cytology for eight consecutive days. Adipose tissue-specific BMP4 transgenic mice were generated as previously described (17). To establish the PCOS model on BMP4-TG mice, 6-week-old BMP4-TG mice were injected daily (s.c.) with insulin and hCG for 3 weeks. Briefly, insulin was injected to mice along with twice-daily injections of 0.21 IU hCG. The dosage of insulin was gradually increased from 0.07 IU on day 1 to 0.84 IU on day 11, and maintained at 0.84 IU from the 12th day until the 22nd day. The mice were subjected to further

investigation after administration. All the animal studies were approved by the Animal Care and Use Committee of the Fudan University Shanghai Medical College and followed the National Institute of Health guidelines on the care and use of animals.

Estrous cycle analysis

For eight consecutive days, vaginal cells of the indicated mice were collected via normal saline lavage daily and visualized under light microscopy after Giemsa staining. Briefly, samples with primarily nucleated cells indicated the proestrus stage, primarily cornified epithelial cells indicated the estrus stage, both cornified cells and leukocytes indicated the metestrus stage, and primarily leukocytes indicated the diestrus stage.

Isolation and culture of ovarian TCs and GCs

The TCs and GCs were isolated from the ovaries of 6-week-old mice. The ovaries were freed from the lower back incision, and then isolated from their connective tissues under a stereomicroscope, cleaned for 2 times and then collected in the Lebovitz's L-15 medium (GIBCO, Gaithersburg, MD, USA) with 10% FBS (GIBCO), 100 U/ml penicillin, 0.1 mg/ml streptomycin. The GCs were released by puncturing the follicles with a sterile hypodermic needle, then collected by centrifugation (300 g) for 3 min and cultured in McCoy's 5a medium (GIBCO) with 10% FBS, 100 U/ml penicillin, 0.1 mg/ml streptomycin.

To isolate TCs, remaining ovary tissues after releasing GCs were washed twice and cut up into fragments using scissors in a McCoy's 5a medium containing 4 mg/ml collagenase (Sigma-Aldrich, St. Louis, MO, USA) and were then pipetted to facilitate cell dispersion. The suspension of ovarian fragments was incubated at 37 °C for 60 minutes and pipetted every 5 min. After digestion, the cell suspension was filtered through a 40-µm cell strainer (BD, Basel,

Switzerland) to remove the undigested ovarian fragments. The filtered TC suspension was centrifuged at 300 g for 5 min, and then washed twice and cultured in McCoy's 5a medium. TCs and GCs both were seeded on 24-well plates (5 × 10⁴/ well), and treated with BMP4 (R & D Systems, Minneapolis, MN, USA), testosterone or DHEA (Sigma-Aldrich) as indicated.

Plasmid construct

The mice Smad1 coding sequence was amplified via PCR using the primers as follows: forward, ATAAAGCTTAATGTGACCAGCTTGTTCATTCACAAG, and reverse, ATAGGATCCTTAAGACACGGATGAAATAGGATTGTGGG, and then cloned into Prk7-N-Flag vector using HindIII (5' end) and BamHI (3' end) restriction sites. The mice Smad4 coding sequence was amplified via PCR using the primers as follows: forward, ATAAAGCTTGACAATATGTCTATAACAAATACACC, and reverse, ATAGAATTCTCAGTCTAAAGGCTGTGGGTCCGCAA, and then cloned into Prk7-N-Flag vector using HindIII (5' end) and EcoRI (3' end) restriction sites. The Flag-tag was added to N-terminal of Smad1 and Smad4. The promoter regions of mouse *BMP4* was amplified via PCR using the primers as follows: forward, CGGAGCTCGGCCAAAGGTCACCTTATTGT C, and reverse, CGCTCGAGTGCCGAACCTCACCTAGCTTC, and then cloned into pGL4.20 luciferase vector (Promega Corp., Madison, WI, USA) using SacI (5' end) and XhoI (3' end) restriction sites. The promoter regions of mouse *CYP17A1* was amplified via PCR using the primers as follows: forward, ATAACGCGTGGCCATAGTGTTCATAGCCCAGGGTGA, and reverse, ATAAGATCTGCAGAGAAGGAGAACTTTTAAAGGC, and then cloned into pGL3-basic luciferase vector (Promega) using MluI (5' end) and BglII (3' end) restriction sites. All the

plasmid constructs were verified by DNA sequencing.

RNA isolation, quantitative PCR (qPCR) and RT-PCR

Total RNA of the cells and tissues was extracted using TRIzol reagent (Invitrogen, Carlsbad, CA, USA). The purified RNA was then subjected to reverse transcription using the PrimeScript reverse transcriptase kit (TaKaRa Bio, Otsu, Japan), followed by qPCR assay. qPCR was carried out using Power SYBR green PCR master mix (Applied Biosystems, Foster City, CA, USA) and a Prism 7500 instrument (Applied Biosystems), with 18S rRNA as an endogenous control. Analysis was done in triplicate and repeated at least 3 times. Results were presented as means and standard deviations (SD) from several independent samples. Forward and reverse primers (5' to 3') of qPCR were listed as follows:

<i>BMP4</i> ,	TTCCTGGTAACCGAATGCTGA	and
	CCTGAATCTCGGCGACTTTTT;	<i>AR</i> ,
	CTGGGAAGGGTCTACCCAC	and
	GGTGCTATGTTAGCGGCCTC;	<i>CYP11A</i> ,
	AGGTCCTTCAATGAGATCCCTT	and
	TCCCTGTAAATGGGGCCATAC;	<i>HSD3B2</i> ,
	GGTTTTTGGGGCAGAGGATCA	and
	GGTACTGGGTGTCAAGAATGTCT;	
<i>CYP17A1</i> ,	GCCCAAGTCAAAGACACCTAAT	
and	GTACCCAGGCGAAGAGAATAGA;	
<i>CYP19A1</i> ,	ATGTTCTTGGAATGCTGAACCC	
and	AGGACCTGGTATTGAAGACGAG;	<i>SF1</i> ,
	AGGTGTCTGGGCTACCACTAC	and
	CCACCCCGCATTCGATCAG;	<i>18S rRNA</i> ,
	CGGCTACCACATCCAAGGAA	and
	GCTGGAATTACCGCGGCT.	

Primers used to detect BMP family members and BMP antagonists were listed in supplemental Table 1. Additionally, RT-PCR was used to detect BMP receptors using specific primers. Forward and reverse primers (5' to 3') of RT-PCR were listed as follows:

<i>Bmpr1a</i> ,	GCGAACTATTGCCAAACAG	and
-----------------	---------------------	-----

GAGGTGGCACAGACCACAAG;
GAACTCCCATTCCTCATC
GCTATTGTCCTTTGGACCAG;
AATCAAGAACGGCTGTGTGCA
CATGCTGTGAAGACCCTGTTT;
CGAAGCCACCCTATTACAAC
ATTAGCCACAGGTCCACATC;
ACCCCAGGTGTACTTCTG
CATGGCCGTAGGGAGGTTTC.

Bmpr1b,
and
Bmpr2,
and
Acvr2a,
and
Acvr2b,
and

The sequences (5' to 3') for shRNAs were shBMP4:
CACCGGATTACATGAGGGATCTTTACGAAT
AAAGATCCCTCATGTAATCC; and shLacZ:
CACCGCTACACAAATCAGCGATTTCGAAA
AATCGCTGATTGTGTAG. Recombinant
adenovirus was produced and amplified in 293A
cells. Then the adenovirus was used to infect
TCs and GCs to disrupt BMP4 expression.

Western blot and antibodies

The cells and tissues were lysed with lysis buffer containing 2% sodium dodecyl sulfate (SDS), 50 mM Tris-HCl (pH 6.8), 10 mM dithiothreitol, 10% glycerol, 0.002% bromophenol blue, phosphatase inhibitors (10 mM Na₃VO₄, 10 mM NaF) and protease inhibitor mixture (Roche, Basel, Switzerland). After quantification, equal amounts of protein were separated by SDS-PAGE, transferred to a polyvinylidene difluoride membrane (Millipore Corp., Bedford, MA). After blocking in 5% bovine serum albumin or non-fat milk, the membrane was immunoblotted with primary antibodies, and visualized with horseradish peroxidase-coupled secondary antibodies (Jackson). The antibodies used in current study were as follows: antibody against BMP4 (MAB1049) was from Millipore; CYP17A1 (ab125022) was from abcam; Flag (F1804) was from Sigma; CYP19A1 (sc-30086), and HSP90 (sc-7947) were from Santa Cruz (CA, USA); p-Smad1/5/8 (#9511), p-p38 MAPK (#9216S), Smad1 (#6944), Smad4 (#9515), p38 MAPK (#9212S) were from cell signaling technology (Danvers, MA, USA).

Generation of recombinant adenovirus

Recombinant adenovirus for BMP4 knockdown was produced through BLOCK-iT Adenoviral RNAi Expression System (Invitrogen) as previously described (35). The adenoviral expression vector pAd/BLOCK-iT encoding short hairpin RNA (shRNA) of BMP4 was constructed, with shRNA for LacZ as the control.

RNA interference

Synthetic stealth siRNA oligonucleotides specific for *AR*, *Smad4*, and *p38 MAPK* mRNA were designed and synthesized by Invitrogen. Two sets of siRNA were used to disrupt expression of Smad4 and p38 MAPK. Stealth siRNA Negative Control (siNC) Duplexes with a similar GC content were used as controls. TCs or GCs were transfected with the siRNA oligonucleotide by using Lipofectamine RNAiMAX (Invitrogen) at 50% confluence as previously described (35-36). The sequences for siRNAs were as follows: siAR: GCAAGUGCCCAAGAUCUUTT; siSmad4-1: CAUACACACCUGAAUUGCCUCACCA; siSmad4-2: CACCUGGAAUUGAUCUCUCAGGAUU; sip38 MAPK-1: CCUUUGAAAGCAGGGACCUUCUCAU; sip38 MAPK-2: CCAGCAACCUAGCUGUGAACGAAGA.

ChIP

TCs and GCs were treated with or without testosterone for 24 h and then subjected to ChIP assay. ChIP was conducted as previously described (35) using anti-AR antibody (Abcam; ab74272), with rabbit IgG as a negative control. Immunoprecipitated DNA was purified and quantified by qPCR, with the DNA level in input sample as an endogenous control. The data were normalized to IgG controls in each group. The primer (5' to 3') for ChIP-qPCR was as follows: BMP4 promoter:

AAACTCAGGGAAGCCCAGAC and
GACCGATGCCTCCAGCTC.

Measurement of total testosterone and estradiol

The levels of total testosterone and estradiol in mice serum and cell culture supernatant were measured by chemiluminescence immunoassay using Beckman coulter unice1 Dxi800 immunology analyzer.

Luciferase reporter assays

The promoter of CYP17A1 and BMP4 region were cloned into the luciferase vector (Promega) as described above. In luciferase reporter assays, 293T cells were transfected in triplicate with

luciferase vector and the indicated transcription factors using the transfection kit Lipofectamine 2000 (Invitrogen) following the manufacturer's instructions. At the 36th hour after transfection, luciferase activity was measured using the dual-luciferase reporter assay (Promega), normalizing the firefly luciferase activity against Renilla luciferase activity.

Statistics

All experiments were independently repeated at least three times, with data presented as means \pm SD. *P* values were determined by unpaired two-tailed Student's *t* test. Differences were considered as significant when *P* < 0.05.

Acknowledgements

We thank Ya-xin Zhao (Fudan University) for assisting with generation of BMP4-Luc reporter plasmid; Rui Sun (Fudan University) for providing AR expression vector.

This research is supported partially by National Key Basic Research Project Grant 2011CB910201 and 2013CB530601, The State Key Program of National Natural Science Foundation 31030048C120114 and 81390350 (to Q.Q.T.); National Natural Science Foundation of China Grant 81601251 and Project funded by China Postdoctoral Science Foundation (to Y.L.); National Key Basic Research Project Grant 2016YFC1303100 (to C.J.X).

Conflict of interest

The authors declare that they have no conflicts of interest with the contents of this article.

Author contributions: Y.L. and S.Y.D. designed and conducted the experiments, analyzed data, and wrote the manuscript. M.D., X.D., F.F.Z. and Z.Y.W. participated in carrying out the experiments *in vivo*. S.W.Q. participated in generation of recombinant adenovirus. M.D., Z.Y.W., S.W.Q. and W.Z. reviewed the manuscript and offered critical advice. Q.Q.T. and C.J.X directed the project and reviewed the manuscript. All authors reviewed the results and approved the final version of the manuscript.

The abbreviations used are: PCOS, polycystic ovary syndrome; BMP4, bone morphogenetic protein 4; DHEA, dehydroepiandrosterone; TCs, theca cells; LH, luteinizing hormone; GCs, granulosa cells; Smad, mothers against dpp; MAPK, mitogen-activated protein kinase; R-Smads, receptor-regulated Smads; coSmad, common partner Smad; TAK1, TGF-beta activated kinase 1; MKK, MAPK kinase kinase; AR, androgen receptor; NCoR, nuclear receptor corepressor; SMRT; silencing mediator of retinoid and thyroid hormone receptors

Reference

1. Azziz, R., Carmina, E., Chen, Z., Dunaif, A., Laven, J. S., Legro, R. S., Lizneva, D., Natterson-Horowitz, B., Teede, H. J., and Yildiz, B. O. (2016) Polycystic ovary syndrome. *Nat Rev Dis Primers* **2**, 16057
2. Rosenfield, R. L., and Ehrmann, D. A. (2016) The Pathogenesis of Polycystic Ovary Syndrome (PCOS): The Hypothesis of PCOS as Functional Ovarian Hyperandrogenism Revisited. *Endocr Rev* **37**, 467-520
3. Palomba, S., and La Sala, G. B. (2016) Pregnancy complications in women with polycystic ovary syndrome: importance of diagnostic criteria or of phenotypic features? *Hum Reprod* **31**, 223-224
4. Deplewski, D., and Rosenfield, R. L. (2000) Role of hormones in pilosebaceous unit development. *Endocr Rev* **21**, 363-392
5. Lizneva, D., Gavrilova-Jordan, L., Walker, W., and Azziz, R. (2016) Androgen excess: Investigations and management. *Best Pract Res Clin Obstet Gynaecol* **37**, 98-118
6. Luque-Ramirez, M., and Escobar-Morreale, H. F. (2015) Targets to treat androgen excess in polycystic ovary syndrome. *Expert Opin Ther Targets* **19**, 1545-1560
7. Miller, W. L., and Auchus, R. J. (2011) The molecular biology, biochemistry, and physiology of human steroidogenesis and its disorders. *Endocr Rev* **32**, 81-151
8. Steinkampf, M. P., Mendelson, C. R., and Simpson, E. R. (1987) Regulation by follicle-stimulating hormone of the synthesis of aromatase cytochrome P-450 in human granulosa cells. *Mol Endocrinol* **1**, 465-471
9. Shohat-Tal, A., Sen, A., Barad, D. H., Kushnir, V., and Gleicher, N. (2015) Genetics of androgen metabolism in women with infertility and hypoandrogenism. *Nat Rev Endocrinol* **11**, 429-441
10. Escobar-Morreale, H., Pazos, F., Potau, N., Garcia-Robles, R., Sancho, J. M., and Varela, C. (1994) Ovarian suppression with triptorelin and adrenal stimulation with adrenocorticotropin in functional hyperandrogenism: role of adrenal and ovarian cytochrome P450c17 alpha. *Fertil Steril* **62**, 521-530
11. Wickenheisser, J. K., Nelson-DeGrave, V. L., Quinn, P. G., and McAllister, J. M. (2004) Increased cytochrome P450 17alpha-hydroxylase promoter function in theca cells isolated from patients with polycystic ovary syndrome involves nuclear factor-1. *Mol Endocrinol* **18**, 588-605
12. Katagiri, T., and Watabe, T. (2016) Bone Morphogenetic Proteins. *Cold Spring Harb Perspect Biol* **8**
13. Wu, M., Chen, G., and Li, Y. P. (2016) TGF-beta and BMP signaling in osteoblast, skeletal development, and bone formation, homeostasis and disease. *Bone Res* **4**, 16009
14. Bragdon, B., Moseychuk, O., Saldanha, S., King, D., Julian, J., and Nohe, A. (2011) Bone morphogenetic proteins: a critical review. *Cell Signal* **23**, 609-620
15. Huang, H., Song, T. J., Li, X., Hu, L., He, Q., Liu, M., Lane, M. D., and Tang, Q. Q. (2009) BMP signaling pathway is required for commitment of C3H10T1/2 pluripotent stem cells to the adipocyte lineage. *Proc Natl Acad Sci U S A* **106**, 12670-12675
16. Tang, Q. Q., and Lane, M. D. (2012) Adipogenesis: from stem cell to adipocyte. *Annu*

17. Qian, S. W., Tang, Y., Li, X., Liu, Y., Zhang, Y. Y., Huang, H. Y., Xue, R. D., Yu, H. Y., Guo, L., Gao, H. D., Sun, X., Li, Y. M., Jia, W. P., and Tang, Q. Q. (2013) BMP4-mediated brown fat-like changes in white adipose tissue alter glucose and energy homeostasis. *Proc Natl Acad Sci U S A* **110**, E798-807
18. Moran, L. J., Norman, R. J., and Teede, H. J. (2015) Metabolic risk in PCOS: phenotype and adiposity impact. *Trends Endocrinol Metab* **26**, 136-143
19. Nilsson, E. E., and Skinner, M. K. (2003) Bone morphogenetic protein-4 acts as an ovarian follicle survival factor and promotes primordial follicle development. *Biol Reprod* **69**, 1265-1272
20. Glistler, C., Richards, S. L., and Knight, P. G. (2005) Bone morphogenetic proteins (BMP) -4, -6, and -7 potently suppress basal and luteinizing hormone-induced androgen production by bovine theca interna cells in primary culture: could ovarian hyperandrogenic dysfunction be caused by a defect in thecal BMP signaling? *Endocrinology* **146**, 1883-1892
21. Dooley, C. A., Attia, G. R., Rainey, W. E., Moore, D. R., and Carr, B. R. (2000) Bone morphogenetic protein inhibits ovarian androgen production. *J Clin Endocrinol Metab* **85**, 3331-3337
22. Erickson, G. F., and Shimasaki, S. (2003) The spatiotemporal expression pattern of the bone morphogenetic protein family in rat ovary cell types during the estrous cycle. *Reprod Biol Endocrinol* **1**, 9
23. Davey, R. A., and Grossmann, M. (2016) Androgen Receptor Structure, Function and Biology: From Bench to Bedside. *Clin Biochem Rev* **37**, 3-15
24. Li, D., Urs, A. N., Allegood, J., Leon, A., Merrill, A. H., Jr., and Sewer, M. B. (2007) Cyclic AMP-stimulated interaction between steroidogenic factor 1 and diacylglycerol kinase theta facilitates induction of CYP17. *Mol Cell Biol* **27**, 6669-6685
25. Groppe, J., Greenwald, J., Wiater, E., Rodriguez-Leon, J., Economides, A. N., Kwiatkowski, W., Affolter, M., Vale, W. W., Izpisua Belmonte, J. C., and Choe, S. (2002) Structural basis of BMP signalling inhibition by the cystine knot protein Noggin. *Nature* **420**, 636-642
26. Li, H., Chen, Y., Yan, L. Y., and Qiao, J. (2013) Increased expression of P450scc and CYP17 in development of endogenous hyperandrogenism in a rat model of PCOS. *Endocrine* **43**, 184-190
27. Sirmans, S. M., and Pate, K. A. (2013) Epidemiology, diagnosis, and management of polycystic ovary syndrome. *Clin Epidemiol* **6**, 1-13
28. Diaz, R. (2011) Reproductive endocrinology: Benefits of metformin in PCOS. *Nat Rev Endocrinol* **7**, 437
29. Matsumoto, T., Sakari, M., Okada, M., Yokoyama, A., Takahashi, S., Kouzmenko, A., and Kato, S. (2013) The androgen receptor in health and disease. *Annu Rev Physiol* **75**, 201-224
30. van de Wijngaart, D. J., Dubbink, H. J., van Royen, M. E., Trapman, J., and Jenster, G. (2012) Androgen receptor coregulators: recruitment via the coactivator binding groove. *Mol Cell Endocrinol* **352**, 57-69
31. Perissi, V., Jepsen, K., Glass, C. K., and Rosenfeld, M. G. (2010) Deconstructing

- repression: evolving models of co-repressor action. *Nat Rev Genet* **11**, 109-123
32. Hodgson, M. C., Astapova, I., Cheng, S., Lee, L. J., Verhoeven, M. C., Choi, E., Balk, S. P., and Hollenberg, A. N. (2005) The androgen receptor recruits nuclear receptor CoRepressor (N-CoR) in the presence of mifepristone via its N and C termini revealing a novel molecular mechanism for androgen receptor antagonists. *J Biol Chem* **280**, 6511-6519
 33. Yu, C., Zhang, Y. L., and Fan, H. Y. (2013) Selective Smad4 knockout in ovarian preovulatory follicles results in multiple defects in ovulation. *Mol Endocrinol* **27**, 966-978
 34. Glistler, C., Kemp, C. F., and Knight, P. G. (2004) Bone morphogenetic protein (BMP) ligands and receptors in bovine ovarian follicle cells: actions of BMP-4, -6 and -7 on granulosa cells and differential modulation of Smad-1 phosphorylation by follistatin. *Reproduction* **127**, 239-254
 35. Liu, Y., Ge, X., Dou, X., Guo, L., Zhou, S. R., Wei, X. B., Qian, S. W., Huang, H. Y., Xu, C. J., Jia, W. P., Dang, Y. J., Li, X., and Tang, Q. Q. (2015) Protein Inhibitor of Activated STAT 1 (PIAS1) Protects Against Obesity-Induced Insulin Resistance by Inhibiting Inflammation Cascade in Adipose Tissue. *Diabetes* **64**, 4061-4074
 36. Liu, Y., Zhang, Y. D., Guo, L., Huang, H. Y., Zhu, H., Huang, J. X., Zhou, S. R., Dang, Y. J., Li, X., and Tang, Q. Q. (2013) Protein inhibitor of activated STAT 1 (PIAS1) is identified as the SUMO E3 ligase of CCAAT/enhancer-binding protein beta (C/EBPbeta) during adipogenesis. *Mol Cell Biol* **33**, 4606-4617

Figure and figure legend

Figure 1

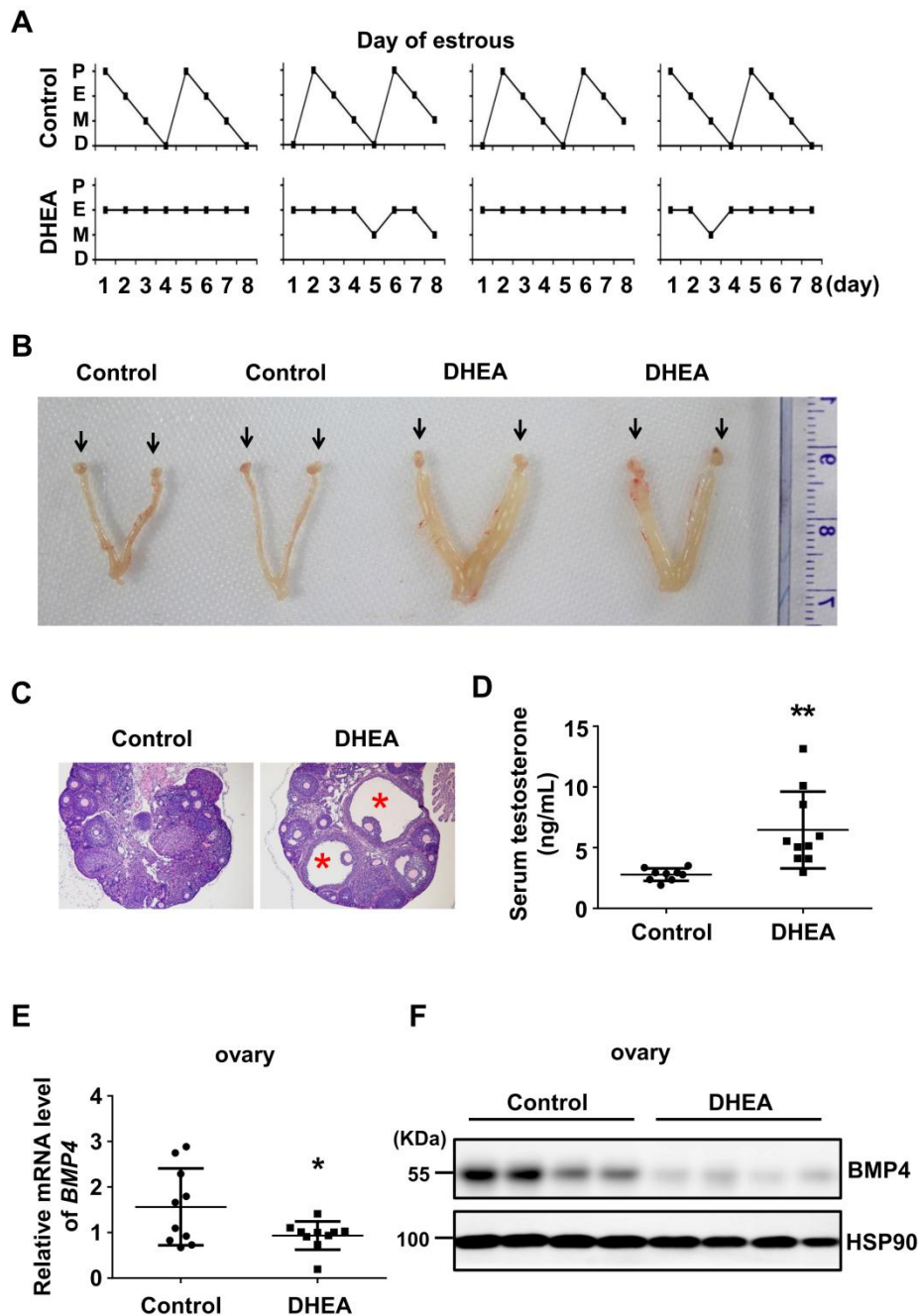


Figure 1. BMP4 was suppressed in the ovary of hyperandrogenism

PCOS hyperandrogenism model was established by injecting DHEA in female 4-week-old mice (n=9-10/group). (A). Estrous cycle was assessed by vaginal cytology for eight consecutive days. Control mice underwent 1-2 estrous cycles, while DHEA-treated mice lost regular estrous cycle. P, proestrus; E, estrus; M, metestrus; D, diestrus. (B). Morphology observation of ovary (arrow) and uterus edema. (C). H&E staining showed cystic follicles (asterisk) in ovary from DHEA-induced mice. (D). Serum total testosterone of control and DHEA-treated mice was measured by chemiluminescence immunoassay. (E). qPCR analysis of

BMP4 mRNA level in the ovaries from control and DHEA-induced mice. (F). Western blot assay of BMP4 protein level in the ovaries of control and DHEA-induced mice, with HSP90 as the loading control. *, $P < 0.05$; **, $P < 0.01$ compared with control group.

Figure 2

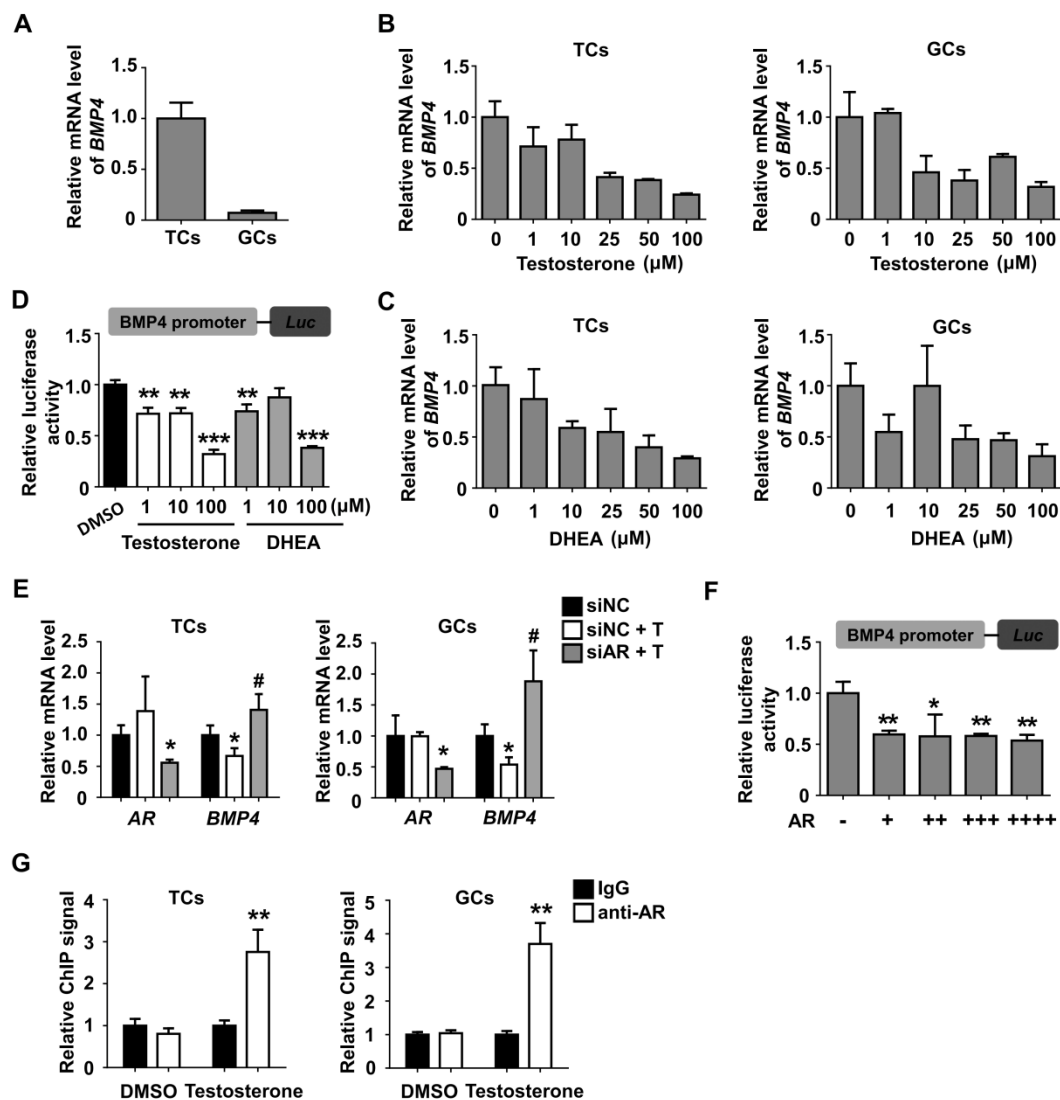


Figure 2. Androgens inhibited BMP4 expression through AR

TCs and GCs were isolated from ovaries of mice as described. (A). qPCR analysis of *BMP4* mRNA levels in TCs and GCs. (B-C). TCs and GCs were treated with testosterone (B) or DHEA (C) at the concentration of 0, 1, 10, 25, 50 and 100 μ M for 48 h. qPCR analysis was used to detect *BMP4* expression. (D). The 293T cells were transfected with *BMP4* promoter and treated with testosterone and DHEA, with DMSO as a control. At the 36th hour after transfection, luciferase activity was measured. The luciferase data were normalized to DMSO-treated cells. (E). TCs and GCs were transfected with siAR to disrupt AR expression, with siNC as control, and then treated with testosterone (25 μ M). qPCR analysis of *AR* and *BMP4* expressions. *, $P < 0.05$ compared with siNC group. #, $P < 0.05$ compared with testosterone-treated siNC group (siNC+T). (F). The 293T cells were transfected with *BMP4*

promoter and AR (0, 0.1, 0.2, 0.3, 0.4 μ g), and then subjected to luciferase measurement at 36th hour after transfection. (G). ChIP-qPCR was conducted in TCs and GCs with or without testosterone treatment for 24 h. Data were normalized to IgG in each group. *, $P < 0.05$; **, $P < 0.01$; ***, $P < 0.001$ compared with control group.

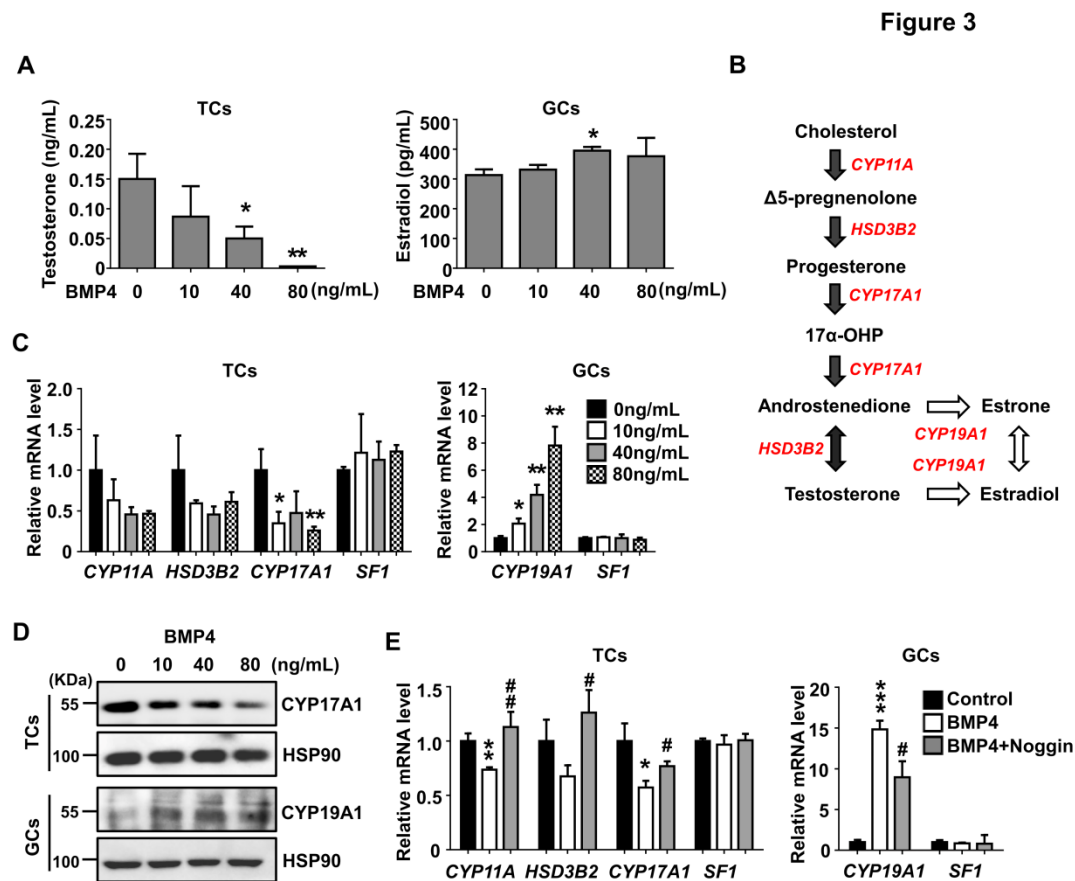
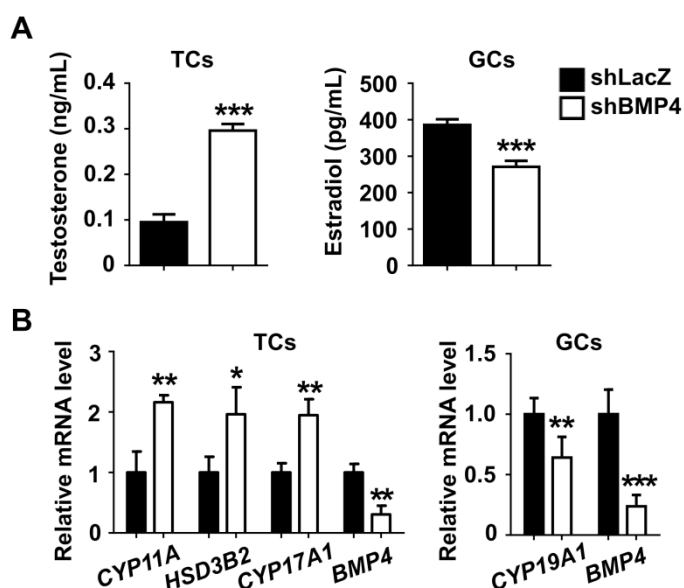
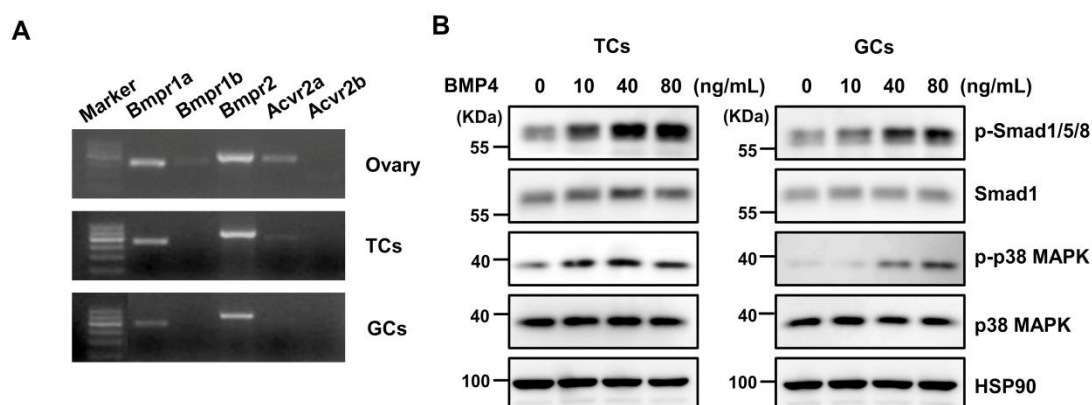


Figure 3. BMP4 controlled synthesis of androgens and estrogens

TCs and GCs were isolated from mice ovaries and treated with BMP4 for 48 h at the concentration of 0, 10, 40 and 80 ng/mL. (A). Testosterone in TCs supernatant and estrogen in GCs supernatant were measured using chemiluminescence immunoassay. (B). Schematic diagram for androgens and estrogens production from cholesterol in ovaries. (C). qPCR analysis of *CYP11A*, *HSD3B2*, *CYP17A1* and *SF1* mRNA levels in TCs (left), and *CYP19A1* and *SF1* mRNA levels in GCs (right) upon BMP4 treatment. (D). Protein level of CYP17A1 in TCs and CYP19A1 in GCs upon BMP4 treatment were detected by western blot. (E). The TCs and GCs were treated with BMP4 (40 ng/mL) and noggin (100 ng/mL) for 48 h as indicated. qPCR analysis of *CYP11A*, *HSD3B2*, *CYP17A1* and *SF1* mRNA levels in TCs (left), and *CYP19A1* and *SF1* mRNA levels in GCs (right). *, $P < 0.05$; **, $P < 0.01$; ***, $P < 0.001$ compared with control group. #, $P < 0.05$; ##, $P < 0.01$ compared with BMP4-treated group.

Figure 4**Figure 4. Knockdown of BMP4 modulated androgen and estrogen levels**

TCs and GCs were isolated from mice ovaries and treated with adenovirus to disrupt BMP4 expression. (A). Testosterone in TCs supernatant and estrogen in GCs supernatant were measured using chemiluminescence immunoassay. (B). qPCR analysis of *CYP11A*, *HSD3B2*, *CYP17A1* and *BMP4* mRNA levels in TCs (left), and *CYP19A1* and *BMP4* mRNA levels in GCs (right) upon BMP4 knockdown. *, $P < 0.05$; **, $P < 0.01$; ***, $P < 0.001$ compared with control group.

Figure 5**Figure 5. BMP4 activated both Smad and p38 MAPK signaling pathway in TCs and GCs**

(A). RT-PCR was used to detect BMP receptors including *Bmpr1a*, *Bmpr1b*, *Bmpr2*, *Acvr2a*, *Acvr2b*,

and *Acvr2b* in mice ovary and isolated TCs and GCs. (B). TCs and GCs were treated with BMP4 at indicated concentration for 3 h, and then subjected to western blot assay for p-Smad1/5/8, Smad1, p-p38 MAPK, p38 MAPK and HSP90.

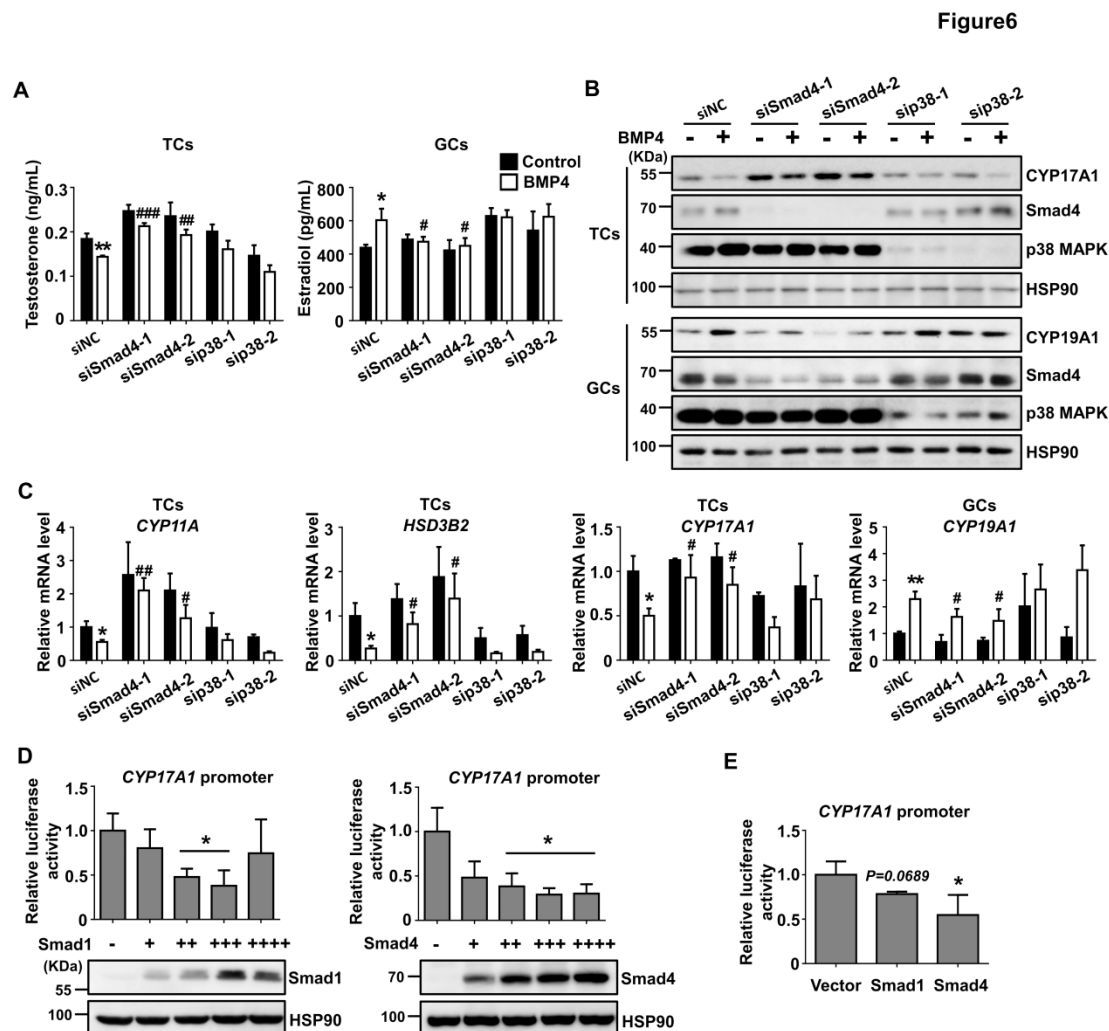


Figure 6. Smad signaling mediated the effect of BMP4 on androgen and estrogen production

Smad4 and p38 MAPK expression in TCs and GCs were respectively disrupted by transfecting two sets of siRNAs, with siNC as control. These cells were then treated with or without BMP4 (40 ng/mL) for 48 h. (A). Testosterone in TCs supernatant and estrogen in GCs supernatant were measured using chemiluminescence immunoassay. (B). Western blot analysis of CYP17A1, CYP19A1, Smad4, p38 MAPK and HSP90 in indicated TCs and GCs. (C). qPCR analysis of *CYP11A*, *HSD3B2*, *CYP17A1* expression in TCs, and *CYP19A1* in GCs. *, $P < 0.05$; **, $P < 0.01$ compared with control group. #, $P < 0.05$; ##, $P < 0.01$; ###, $P < 0.001$ compared with BMP4-treated control group. (D). The 293T cells were transfected with CYP17A1 promoter (0.25 μ g), Flag-Smad1 (left) or Flag-Smad4 (right) at 0, 0.1, 0.2, 0.3, 0.4 μ g. At the

36th hour after transfection, luciferase activity was measured and data were normalized to the cells without Smad transfection. Western blot with Flag antibody was used to detect expression of Flag-Smad1 and Flag-Smad4. (E). TCs were transfected with CYP17A1 promoter (0.3 μ g), Flag-Smad1 (0.3 μ g) or Flag-Smad4 (0.3 μ g). At the 36th hour after transfection, luciferase activity was conducted and data were normalized to the cells without Smad transfection. *, $P < 0.05$

Figure 7

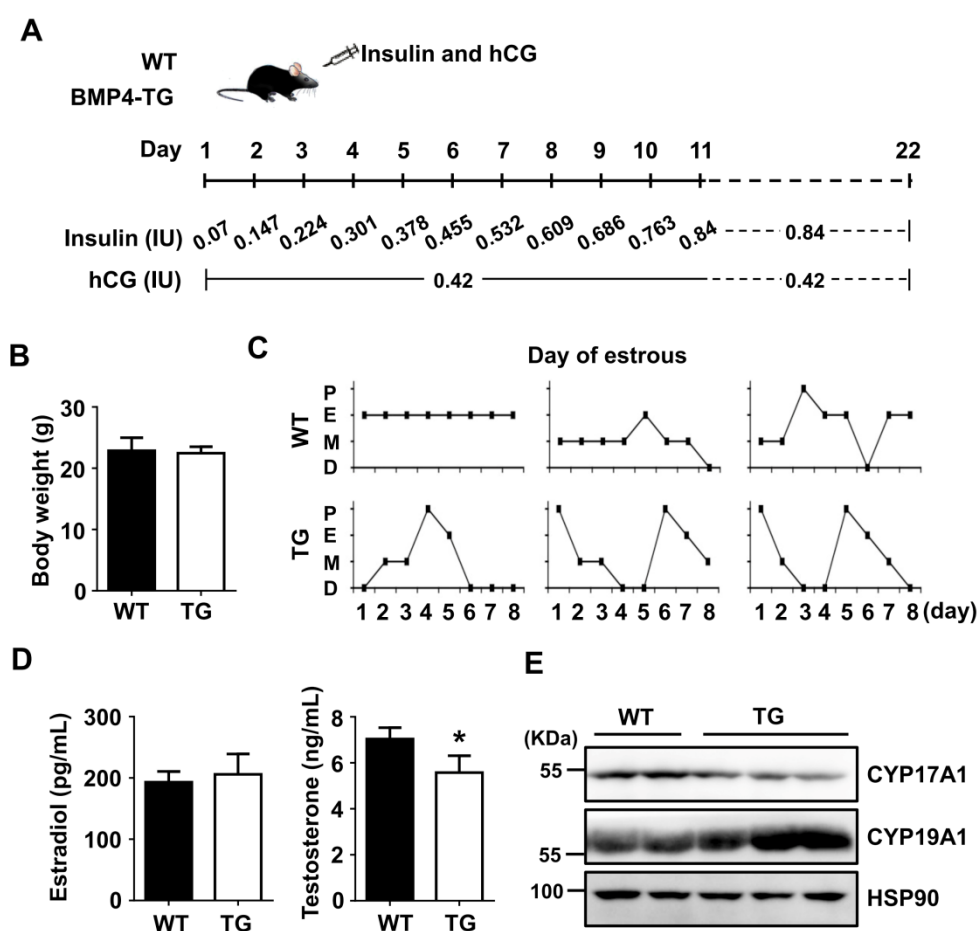


Figure 7. BMP4 inhibited hyperandrogenism occurrence *in vivo*

(A). To establish hyperandrogenism model, the 6-week-old WT and BMP4-TG mice were injected daily (s.c.) with insulin and hCG at the indicated dose for 3 weeks. In brief, the mice were injected with 0.07 IU insulin on day 1, and the dosage was gradually increased to 0.84 IU on day 11. The dosage of insulin was then maintained at 0.84 IU from the 12th day until the 22nd day. The insulin was administered along with twice-daily injections of 0.21 IU hCG. The mice were subjected to further investigation after administration. (B-D). The body weight (B), estrous cycle (C), serum estrogen (left in D) and androgen (right in D) were measured in WT and BMP4-TG mice ($n=3/\text{group}$). (E). Western blot analysis of CYP17A1 and CYP19A1 levels in ovaries of WT and BMP4-TG mice. *, $P < 0.05$

Figure 8

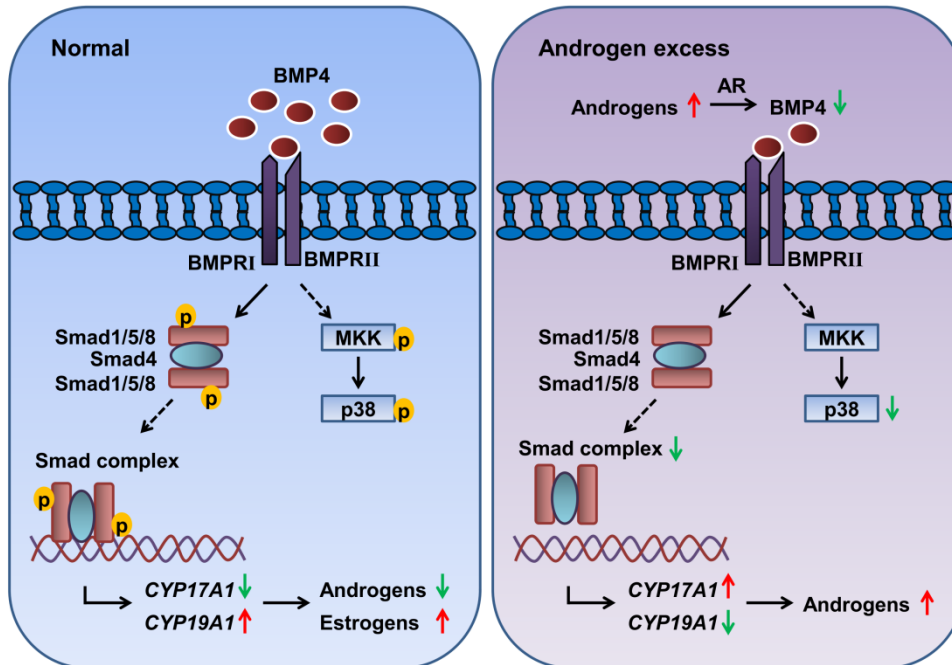


Figure 8. Model of the role of BMP4 in regulating hyperandrogenism development.

In normal, BMP4 inhibited the androgen and promoted estrogen synthesis via Smad signaling in ovary. In the condition of androgen excess, ovarian BMP4 expression was suppressed by activated AR. The negative regulation of androgen synthesis was then relieved as a result of downregulated BMP4, leading to further increase of androgen level. Accordingly, hyperandrogenism eventually developed.

The BMP4-Smad Signaling Pathway Regulates Hyperandrogenism Development in a Female Mouse Model

Yang Liu, Shao-Yue Du, Meng Ding, Xin Dou, Fei-Fei Zhang, Zhi-Yong Wu, Shu-Wen Qian, Wei Zhang, Qi-Qun Tang and Cong-Jian Xu

J. Biol. Chem. published online June 1, 2017

Access the most updated version of this article at doi: [10.1074/jbc.M117.781369](https://doi.org/10.1074/jbc.M117.781369)

Alerts:

- [When this article is cited](#)
- [When a correction for this article is posted](#)

[Click here](#) to choose from all of JBC's e-mail alerts

Supplemental material:

<http://www.jbc.org/content/suppl/2017/06/01/M117.781369.DC1>

This article cites 0 references, 0 of which can be accessed free at

<http://www.jbc.org/content/early/2017/06/01/jbc.M117.781369.full.html#ref-list-1>